Electronic Supplementary Material (ESI) for RSC Advances.

Supporting Information

Porous ZnO-Co_3O_4 Heteronanostructures Derived from Nano Coordination Polymers for Enhanced Gas Sorption and Visible Light Photocatalytic Applications

*Md.Rakibuddin and Rajakumar Ananthakrishnan**

Department of Chemistry, Indian Institute of Technology, Kharagpur 721 302, India.

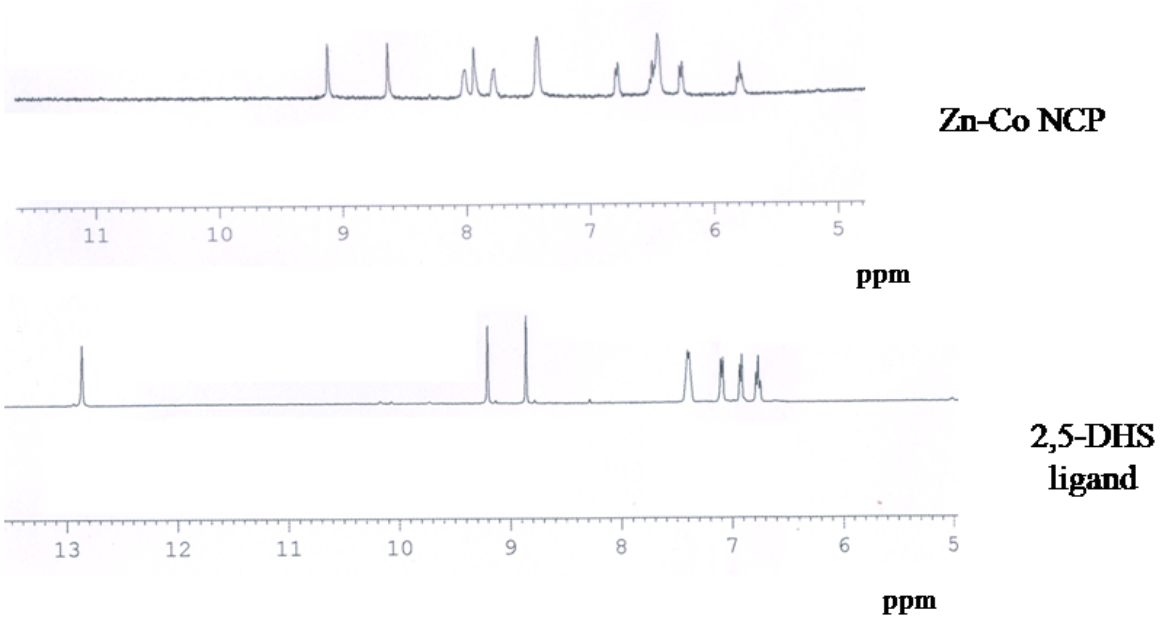

Fig.S1 ^{1}H NMR (400 MHz) spectra of the synthesized Zn-Co NCP and precursor DHS ligand digesting in DMSO-d_6 solvent.

The ^{1}H NMR studies of the Zn-Co NCP 61 and the ligand 2,5-DHS were investigated by digesting the particles in DMSO-d_6. The ^{1}H NMR of the 2,5-DHS shows the peaks of the phenolic –OH group at 12.9 and 9.25 ppm, which are completely vanished in the 2,5-NCP due to coordination of –OH group to the Zn^{+2}. The peaks of the two azomethine hydrogen of the ligand in the NCPs appeared at 8.6 and 9.1 ppm. The aromatic hydrogen of BDC^{2-} incorporated into the NCP appeared between 7.7-8.0 ppm indicating formation of the NCP.[1]

1. S. Jung, W. Cho, H. J. Lee and M. Oh, *Angew. Chem. Int. Ed*. 2009, **48**, 1459-1462.

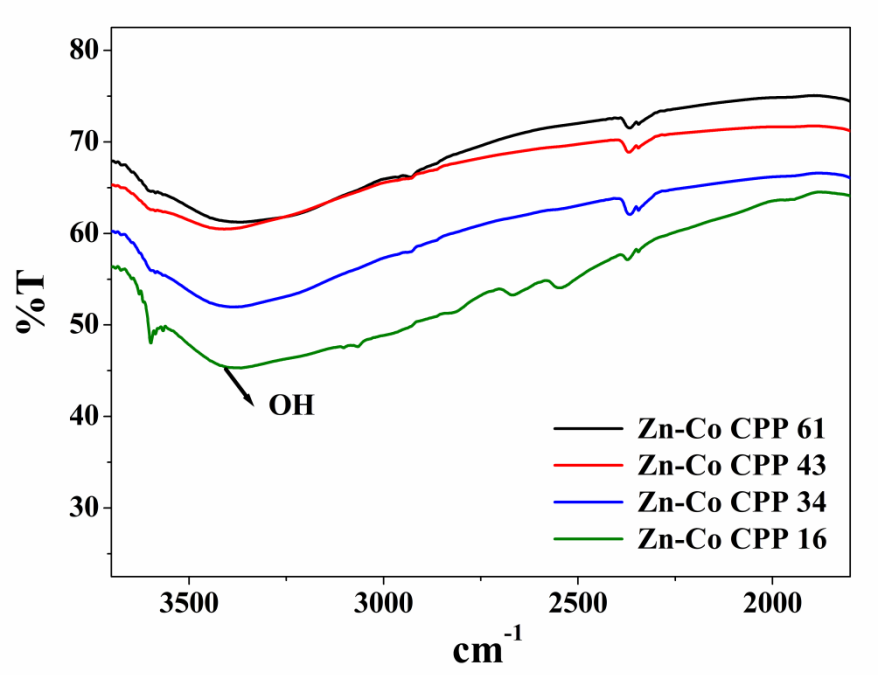

Fig.S2 FT-IR spectra of the prepared NCPs at higher wavenumber (1800-3700 cm^{-1}).

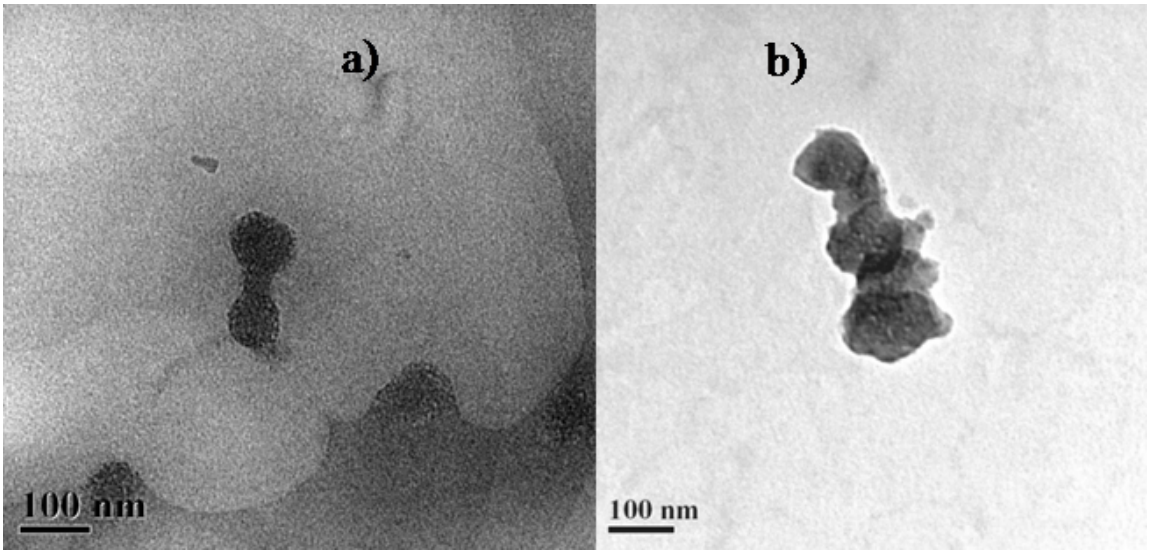

Fig.S3 TEM image of the synthesized a) Zn-Co NCP 43 and b) Zn-Co NCP 16.

The TEM image of the hexagonal lump shaped Zn-Co NCP showing average size about 70-100 nm depending on different ratios.

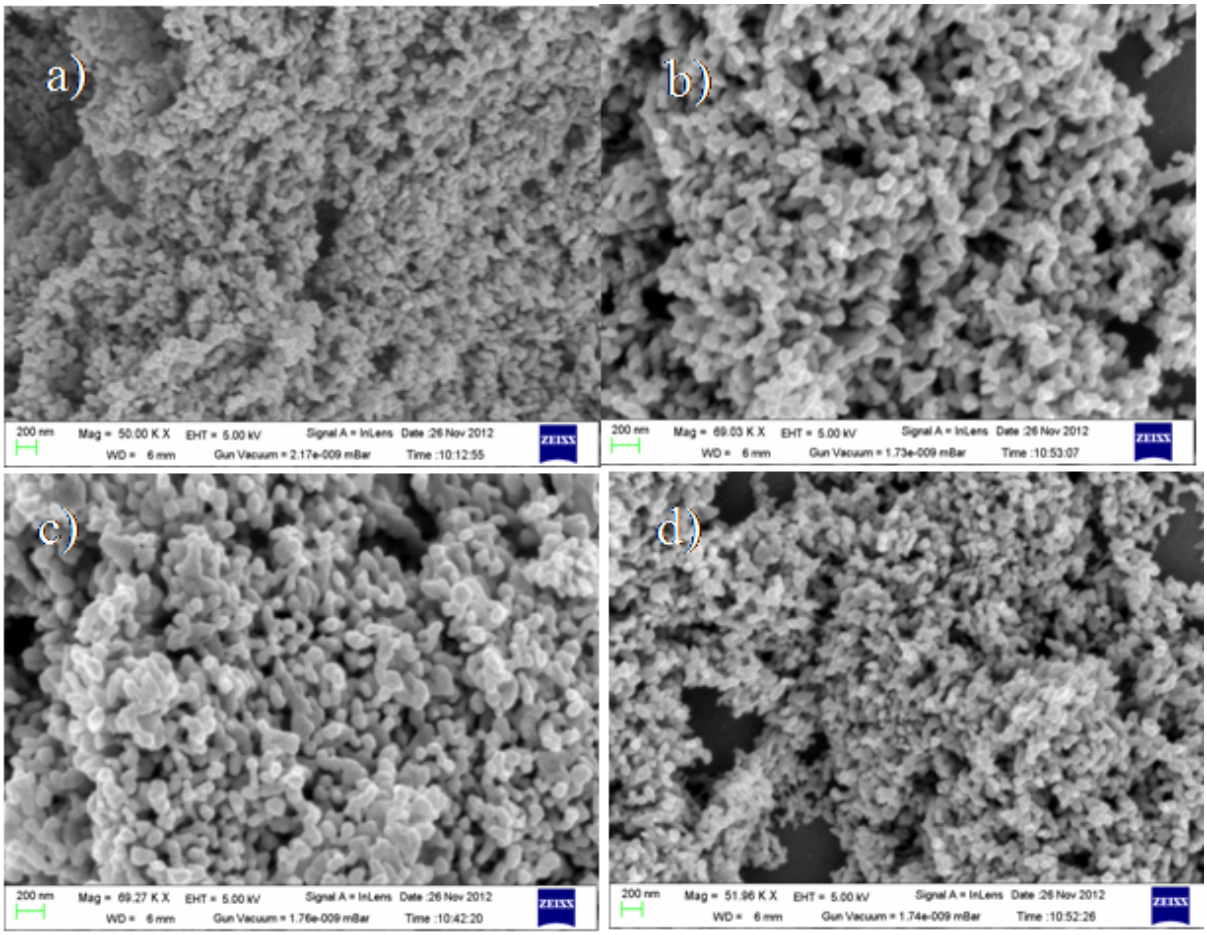

Fig.S4. FESEM image of the obtained ZnO-Co_3O_4 heteronanostructures: a) ZnO-Co_3O_4 61; b) ZnO-Co_3O_4 43, c) ZnO-Co_3O_4 34 and d) ZnO-Co_3O_4 16.

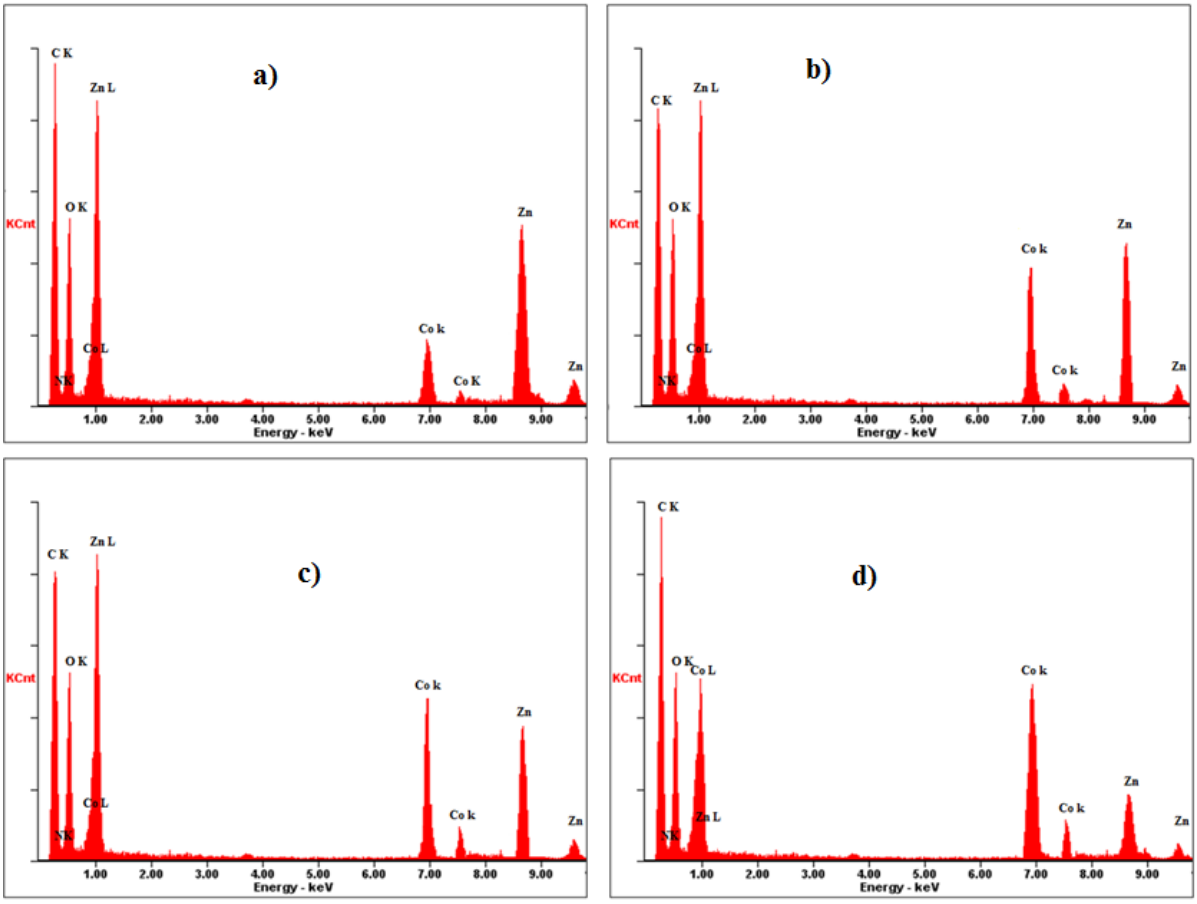

Fig.S5 EDX spectrum of the synthesized Zn-Co NCPs: a) Zn-Co NCP 61, b) Zn-Co NCP 43, c) Zn-Co NCP 34 and d) Zn-Co NCP 16.

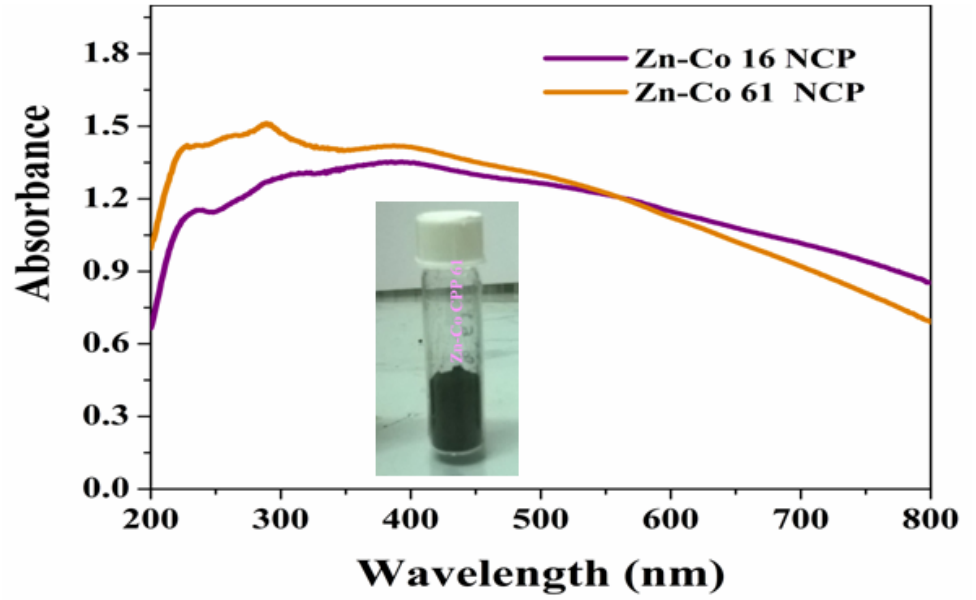

Fig.S6 DRS spectra of the Zn-Co NCPs.

The DRS spectra of the NCPs show broad visible light absorption, and hence the color of the NCPs appears to be black from the two initial colorless precursors.

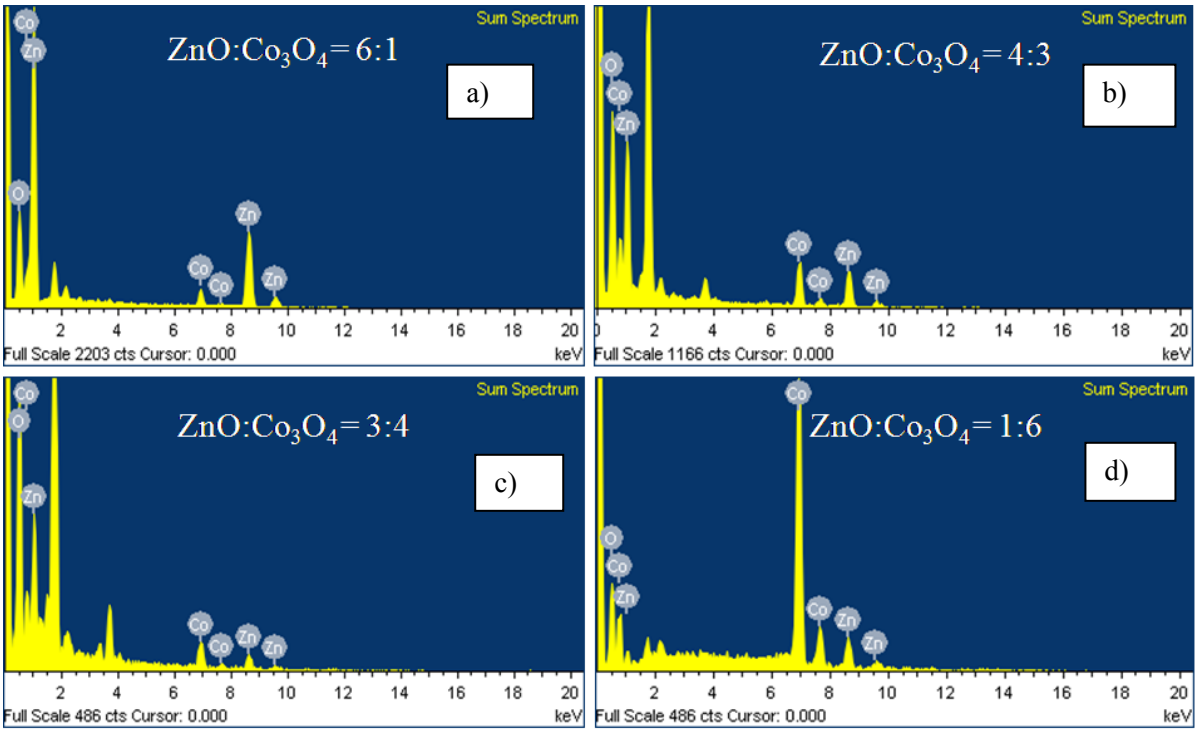

Fig.S7 EDX analysis of the prepared ZnO-Co_3O_4 heterostructures after calcinations of the Zn-Co NCPs at 500 °C, a) ZnO-Co_3O_4 61, b) ZnO-Co_3O_4 43, c) ZnO-Co_3O_4 34 and d) ZnO-Co_3O_4 16.

The EDX analysis shows the presence of Zn, Co and O in the ZnO-Co_3O_4 heteronanostructures. The peak intensity of the Zn and Co is increased or decreased upon changing their ratios.

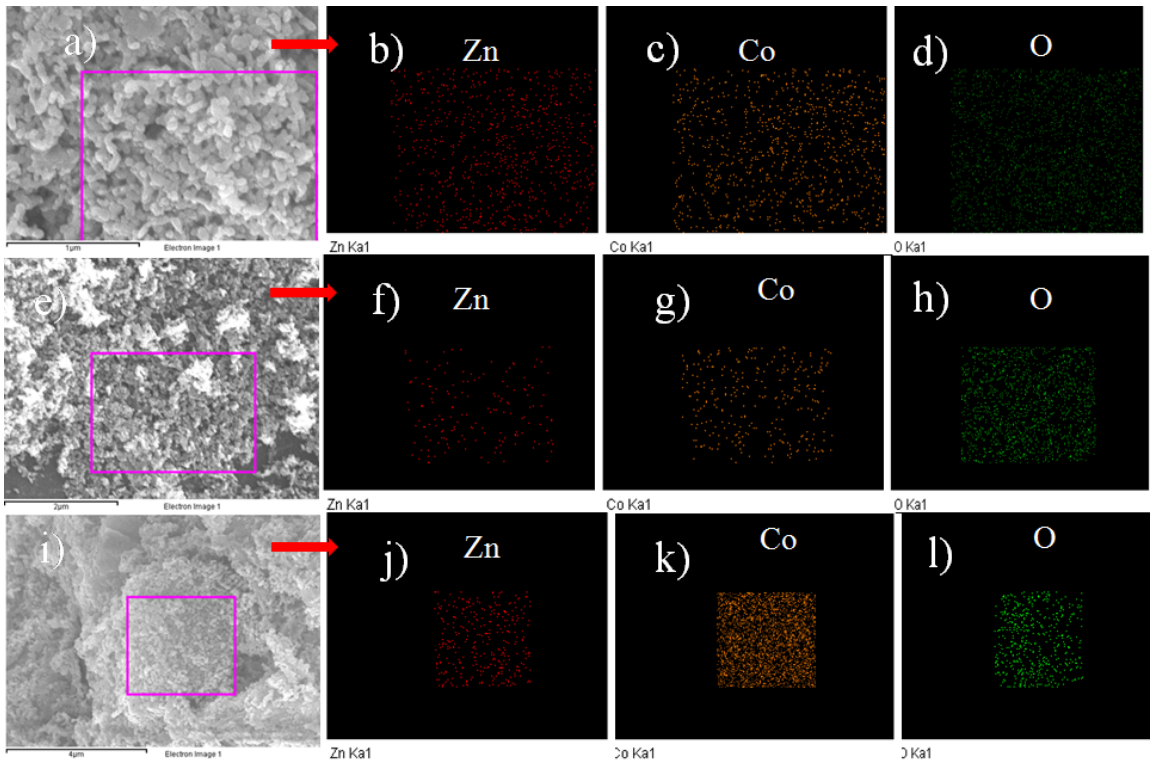

Fig.S8. Elemental area mapping of the Zn, Co, O of the a,b,c,d) ZnO-Co_3O_4 43; e,f,g,h) ZnO-Co_3O_4 34 and i,j,k,l) ZnO-Co_3O_4 16 heterostructures showing the elemental distribution in the respective samples from the FESEM image.

Elemental area mapping is obtained from the corresponding FESEM image of a particular area showing the change in concentration of Zn/ Co upon changing their ratios in the respective nanostructures. Here, Zn (f, j) is in low concentration than Co (g, k) in the ZnO-Co_3O_4 34 and ZnO-Co_3O_4 16 heterostructures.

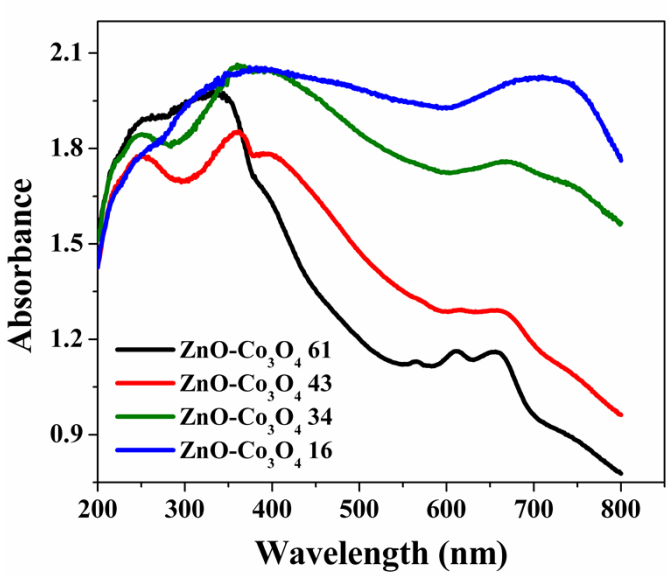

Fig.S9 Diffuse Reflectance Spectra of the synthesized ZnO-Co_3O_4 heteronanostructures.

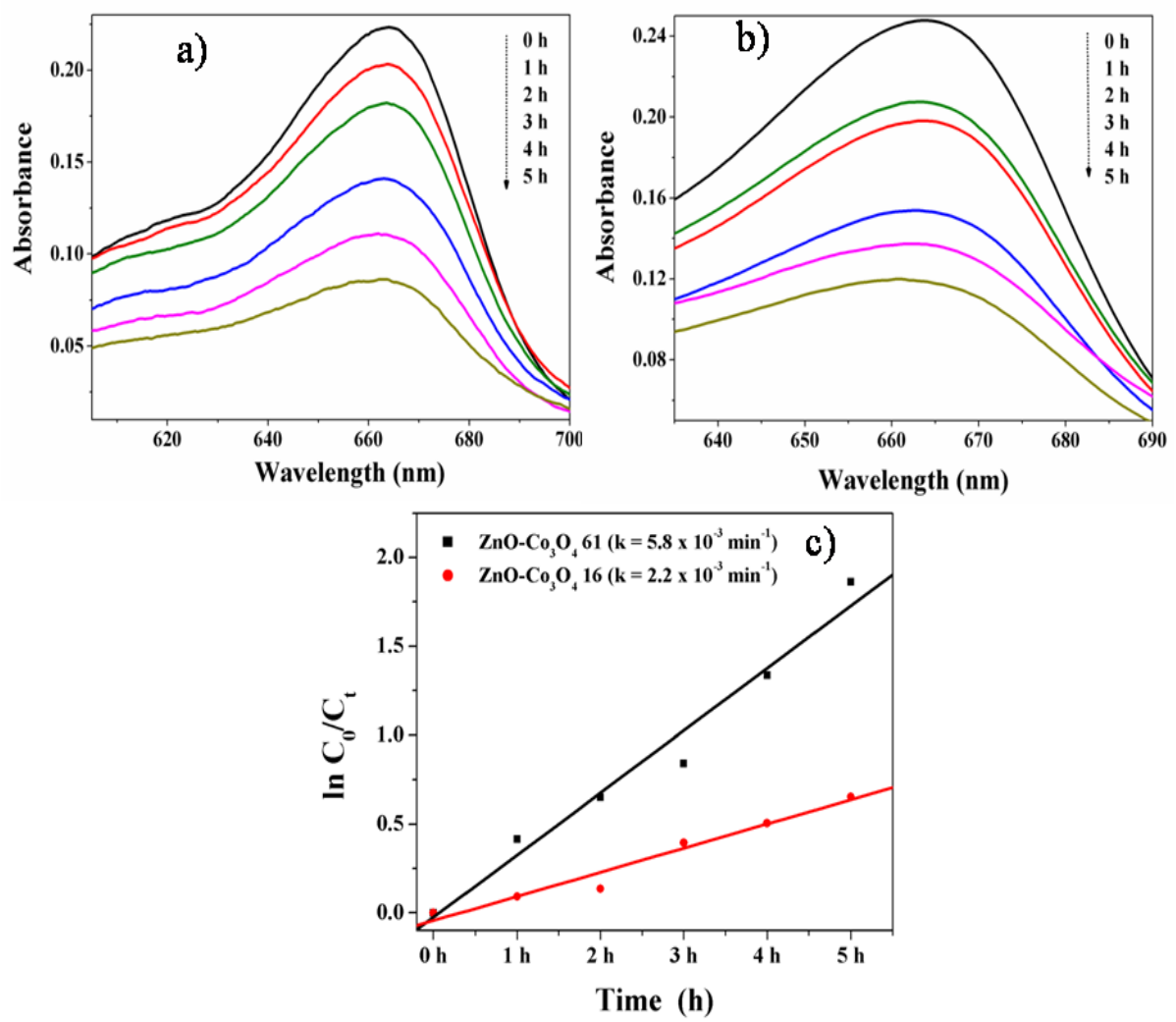

Fig.S10 UV-visible absorption spectra of the degradation of MB dye in presence of a) ZnO-Co_3O_4 43, b) ZnO-Co_3O_4 16 and c) ln C_0/C_t vs time plot for determination of rate constant of the catalyst.

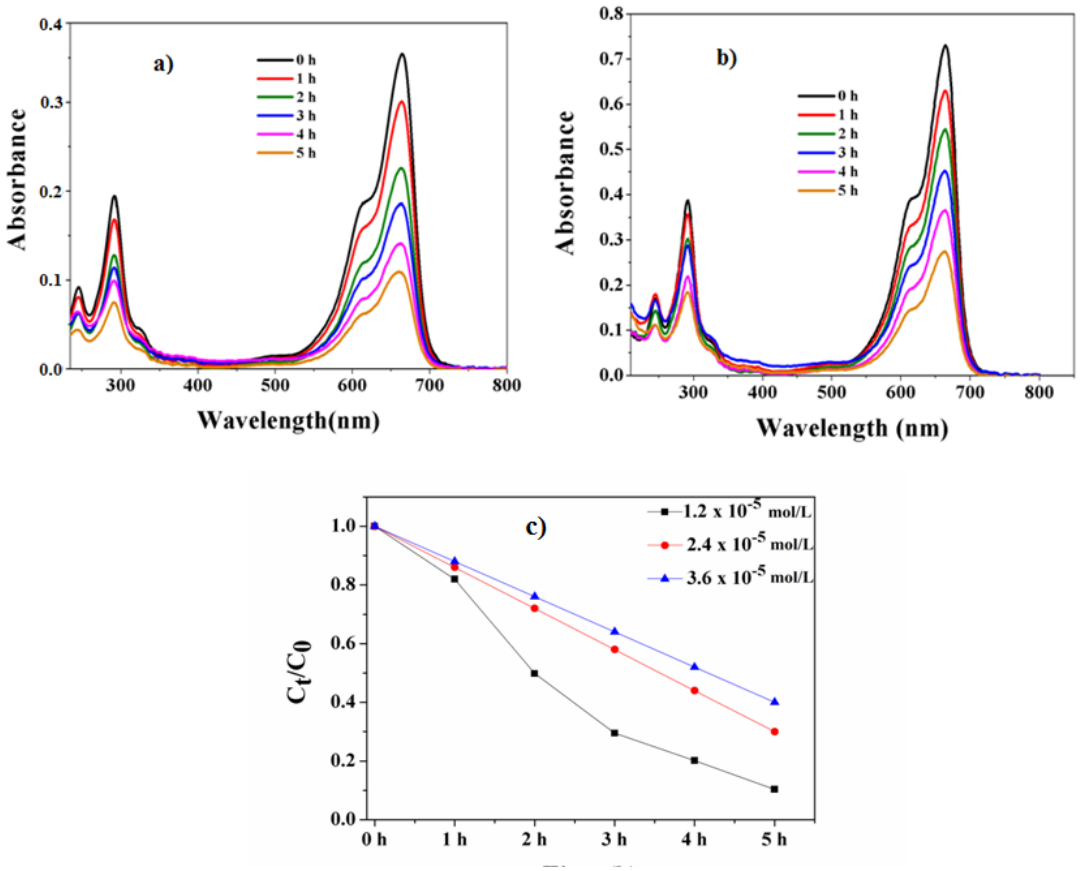

Fig.S11. Effect of concentrations for degradation of MB in presence of ZnO-Co_3O_4 61 catalyst; a) 2.4 x10^{-5} mol/L, b) 3.6 x 10^{-5} mol/L and c) C_t/C_0 vs time plot.

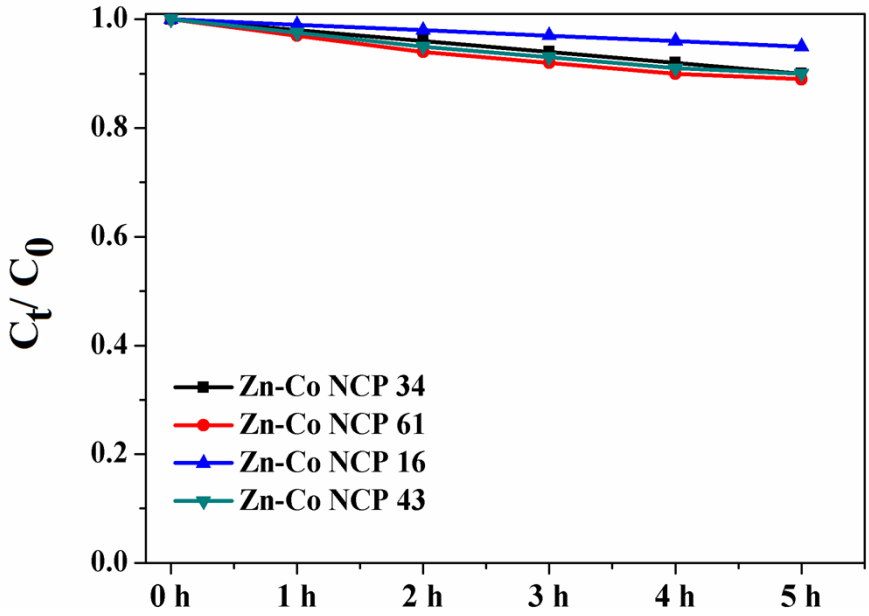

Fig.S12 Degradation kinetics of MB in presence of Zn-Co NCPs

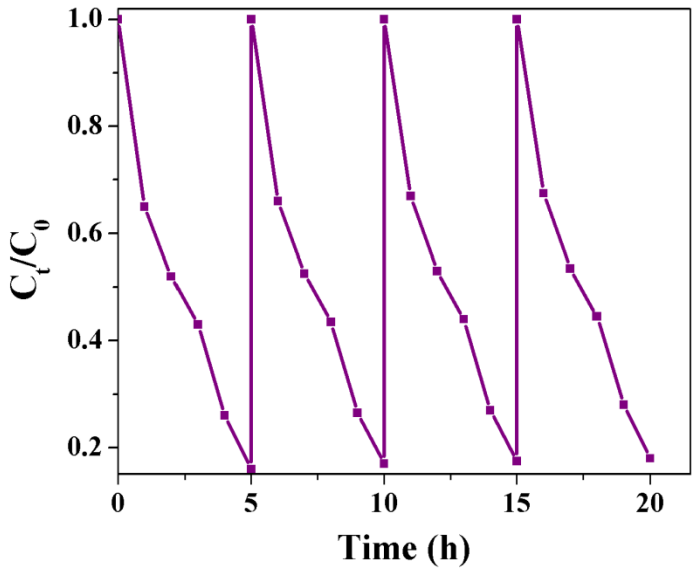

Fig.S13. Reusability study of the ZnO-Co_3O_4 61.

Table S1. BET surface area, pore volume and N_2 gas sorption capacity of the synthesized Zn-Co NCPs and corresponding ZnO-Co_3O_4 heteronanostructures

Sample name	Surface area (m^2/g)	Pore volume (cc/g)	N_2 gas uptake capacity (cc/g)
Zn-Co NCP 61	225.3	0.123	130
Zn-Co NCP 43	202.4	0.103	110
Zn-Co NCP 16	189.3	0.272	295
ZnO-Co_3O_4 61	140.4	0.552	645
ZnO-Co_3O_4 43	110.8	0.366	355
ZnO-Co_3O_4 16	80.5	0.355	345